Measurement of R_b Using a Vertex Mass Tag

K. Abe,[19] K. Abe,[30] T. Akagi,[28] N. J. Allen,[4] W. W. Ash,[28,*] D. Aston,[28] K. G. Baird,[24] C. Baltay,[34] H. R. Band,[33] M. B. Barakat,[34] G. Baranko,[9] O. Bardon,[15] T. L. Barklow,[28] G. L. Bashindzhagyan,[18] A. O. Bazarko,[10] R. Ben-David,[34] A. C. Benvenuti,[2] G. M. Bilei,[22] D. Bisello,[21] G. Blaylock,[16] J. R. Bogart,[28] B. Bolen,[17] T. Bolton,[10] G. R. Bower,[28] J. E. Brau,[20] M. Breidenbach,[28] W. M. Bugg,[29] D. Burke,[28] T. H. Burnett,[32] P. N. Burrows,[15] W. Busza,[15] A. Calcaterra,[12] D. O. Caldwell,[5] D. Calloway,[28] B. Camanzi,[11] M. Carpinelli,[23] R. Cassell,[28] R. Castaldi,[23,†] A. Castro,[21] M. Cavalli-Sforza,[6] A. Chou,[28] E. Church,[32] H. O. Cohn,[29] J. A. Coller,[3] V. Cook,[32] R. Cotton,[4] R. F. Cowan,[15] D. G. Coyne,[6] G. Crawford,[28] A. D'Oliveira,[7] C. J. S. Damerell,[25] M. Daoudi,[28] N. de Groot,[28] R. De Sangro,[12] R. Dell'Orso,[23] P. J. Dervan,[4] M. Dima,[8] D. N. Dong,[15] P. Y. C. Du,[29] R. Dubois,[28] B. I. Eisenstein,[13] R. Elia,[28] E. Etzion,[33] S. Fahey,[9] D. Falciai,[22] C. Fan,[9] J. P. Fernandez,[6] M. J. Fero,[15] R. Frey,[20] T. Gillman,[25] G. Gladding,[13] S. Gonzalez,[15] E. L. Hart,[29] J. L. Harton,[8] A. Hasan,[4] Y. Hasegawa,[30] K. Hasuko,[30] S. J. Hedges,[3] S. S. Hertzbach,[16] M. D. Hildreth,[28] J. Huber,[20] M. E. Huffer,[28] E. W. Hughes,[28] H. Hwang,[20] Y. Iwasaki,[30] D. J. Jackson,[25] P. Jacques,[24] J. A. Jaros,[28] Z. Y. Jiang,[28] A. S. Johnson,[3] J. R. Johnson,[33] R. A. Johnson,[7] T. Junk,[28] R. Kajikawa,[19] M. Kalelkar,[24] H. J. Kang,[26] I. Karliner,[13] H. Kawahara,[28] H. W. Kendall,[15] Y. D. Kim,[26] M. E. King,[28] R. King,[28] R. R. Kofler,[16] N. M. Krishna,[9] R. S. Kroeger,[17] J. F. Labs,[28] M. Langston,[20] A. Lath,[15] J. A. Lauber,[9] D. W. G. S. Leith,[28] V. Lia,[15] M. X. Liu,[34] X. Liu,[6] M. Loreti,[21] A. Lu,[5] H. L. Lynch,[28] J. Ma,[32] G. Mancinelli,[24] S. Manly,[34] G. Mantovani,[22] T. W. Markiewicz,[28] T. Maruyama,[28] H. Masuda,[28] E. Mazzucato,[11] A. K. McKemey,[4] B. T. Meadows,[7] R. Messner,[28] P. M. Mockett,[32] K. C. Moffeit,[28] T. B. Moore,[34] D. Muller,[28] T. Nagamine,[28] S. Narita,[30] U. Nauenberg,[9] H. Neal,[28] M. Nussbaum,[7,*] Y. Ohnishi,[19] N. Oishi,[19] D. Onoprienko,[29] L. S. Osborne,[15] R. S. Panvini,[31] C. H. Park,[27] H. Park,[20] T. J. Pavel,[28] I. Peruzzi,[12,‡] M. Piccolo,[12] L. Piemontese,[11] E. Pieroni,[23] K. T. Pitts,[20] R. J. Plano,[24] R. Prepost,[33] C. Y. Prescott,[28] G. D. Punkar,[28] J. Quigley,[15] B. N. Ratcliff,[28] T. W. Reeves,[31] J. Reidy,[17] P. L. Reinertsen,[6] P. E. Rensing,[28] L. S. Rochester,[28] P. C. Rowson,[10] J. J. Russell,[28] O. H. Saxton,[28] T. Schalk,[6] R. H. Schindler,[28] B. A. Schumm,[6] J. Schwiening,[28] S. Sen,[34] V. V. Serbo,[33] M. H. Shaevitz,[10] J. T. Shank,[3] G. Shapiro,[14] D. J. Sherden,[28] K. D. Shmakov,[29] C. Simopoulos,[28] N. B. Sinev,[20] S. R. Smith,[28] M. B. Smy,[8] J. A. Snyder,[34] H. Staengle,[8] P. Stamer,[24] H. Steiner,[14] R. Steiner,[1] M. G. Strauss,[16] D. Su,[28] F. Suekane,[30] A. Sugiyama,[19] S. Suzuki,[19] M. Swartz,[28] A. Szumilo,[32] T. Takahashi,[28] F. E. Taylor,[15] E. Torrence,[15] A. I. Trandafir,[16] J. D. Turk,[34] T. Usher,[28] J. Va'vra,[28] C. Vannini,[23] E. Vella,[28] J. P. Venuti,[31] R. Verdier,[15] P. G. Verdini,[23] D. L. Wagner,[9] S. R. Wagner,[28] A. P. Waite,[28] S. J. Watts,[4] A. W. Weidemann,[29] E. R. Weiss,[32] J. S. Whitaker,[3] S. L. White,[29] F. J. Wickens,[25] D. C. Williams,[15] S. H. Williams,[28] S. Willocq,[28] R. J. Wilson,[8] W. J. Wisniewski,[28] M. Woods,[28] G. B. Word,[24] J. Wyss,[21] R. K. Yamamoto,[15] J. M. Yamartino,[15] X. Yang,[20] J. Yashima,[30] S. J. Yellin,[5] C. C. Young,[28] H. Yuta,[30] G. Zapalac,[33] R. W. Zdarko,[28] and J. Zhou[20]

(SLD Collaboration)

[1]*Adelphi University, Garden City, New York 11530*
[2]*INFN Sezione di Bologna, I-40126 Bologna, Italy*
[3]*Boston University, Boston, Massachusetts 02215*
[4]*Brunel University, Uxbridge, Middlesex UB8 3PH, United Kingdom*
[5]*University of California at Santa Barbara, Santa Barbara, California 93106*
[6]*University of California at Santa Cruz, Santa Cruz, California 95064*
[7]*University of Cincinnati, Cincinnati, Ohio 45221*
[8]*Colorado State University, Fort Collins, Colorado 80523*
[9]*University of Colorado, Boulder, Colorado 80309*
[10]*Columbia University, New York, New York 10027*
[11]*INFN Sezione di Ferrara and Università di Ferrara, I-44100 Ferrara, Italy*
[12]*INFN Laboratori Nazionali di Frascati, I-00044 Frascati, Italy*
[13]*University of Illinois, Urbana, Illinois 61801*
[14]*E. O. Lawrence Berkeley Laboratory, University of California, Berkeley, California 94720*
[15]*Massachusetts Institute of Technology, Cambridge, Massachusetts 02139*
[16]*University of Massachusetts, Amherst, Massachusetts 01003*
[17]*University of Mississippi, University, Mississippi 38677*
[18]*Moscow State University, Institute of Nuclear Physics 119899 Moscow, Russia*
[19]*Nagoya University, Chikusa-ku, Nagoya 464 Japan*
[20]*University of Oregon, Eugene, Oregon 97403*
[21]*INFN Sezione di Padova and Università di Padova, I-35100 Padova, Italy*

 0031-9007/98/80(4)/660(6)$15.00

[22]*INFN Sezione di Perugia and Università di Perugia, I-06100 Perugia, Italy*
[23]*INFN Sezione di Pisa and Università di Pisa, I-56100 Pisa, Italy*
[24]*Rutgers University, Piscataway, New Jersey 08855*
[25]*Rutherford Appleton Laboratory, Chilton, Didcot, Oxon OX11 0QX United Kingdom*
[26]*Sogang University, Seoul, Korea*
[27]*Soongsil University, Seoul, Korea 156-743*
[28]*Stanford Linear Accelerator Center, Stanford University, Stanford, California 94309*
[29]*University of Tennessee, Knoxville, Tennessee 37996*
[30]*Tohoku University, Sendai 980 Japan*
[31]*Vanderbilt University, Nashville, Tennessee 37325*
[32]*University of Washington, Seattle, Washington 98195*
[33]*University of Wisconsin, Madison, Wisconsin 53706*
[34]*Yale University, New Haven, Connecticut 06511*
(Received 15 August 1997)

We report a new measurement of $R_b = \Gamma_{Z^0\to b\overline{b}}/\Gamma_{Z^0\to\text{hadrons}}$ using a double tag technique, where the b hemisphere selection is based on the reconstructed mass of the B hadron decay vertex. The measurement was performed using a sample of 130×10^3 hadronic Z^0 events, collected with the SLD detector at SLC. The method utilizes the 3D vertexing abilities of the CCD pixel vertex detector and the small stable SLC beams to obtain a high b-tagging efficiency and purity. We obtain $R_b = 0.2142 \pm 0.0034(\text{stat}) \pm 0.0015(\text{syst}) \pm 0.0002(R_c)$. [S0031-9007(97)05018-7]

PACS numbers: 13.38.Dg, 12.15.Ji

We report a new measurement of R_b, the fraction of $Z^0 \to b\overline{b}$ events in hadronic Z^0 decays, collected at the SLAC Linear Collider (SLC) with the SLC Large Detector (SLD), using a mass tag technique. The ratio R_b is of special interest as a test of the standard model (SM), since it is sensitive to possible new physics effects which modify the radiative corrections to $Zb\overline{b}$ vertex. The vertex corrections are isolated because R_b is a ratio between two hadronic rates, hence propagator (oblique), radiative, and QCD corrections common to all quark flavors mostly cancel. Recent measurements yielded a world average R_b value 3σ higher than that predicted by the SM [1]. Previous measurements [2] selected $b\overline{b}$ events based upon mainly the long B hadron lifetime and were limited systematically by contamination in the sample from residual $c\overline{c}$ events. To avoid this limitation our b tag exploits the large B mass, since the mass distribution has a very small charm contamination beyond the charm mass cutoff. Taking advantage of SLD's precise 3D vertexing capability and the small and stable SLC beam spot, we achieve a very efficient and pure b selection. We use a self-calibrating double tag technique [2], which allows one to measure both R_b and the b-tag efficiency, ϵ_b, simultaneously.

This measurement is performed using approximately 130×10^3 $e^+e^- \to Z^0 \to q\overline{q}$ events collected during 1993–1995. A detailed description of the detector can be found elsewhere [3]. We used the information from charged particle tracks measured with the charge-coupled device (CCD) pixel vertex detector (VXD) along with the central drift chamber. The event selection and the determination of the thrust axis use the energy deposits measured with the liquid argon calorimeter.

The luminous region of the SLC interaction point (IP) has a size of about (1.5×0.8) μm in the x-y plane transverse to the beam direction and 700 μm along the beam direction. We use the average IP position of small groups of sequential hadronic events to determine the primary vertex (PV) in the x-y plane. The longitudinal position of the PV is determined for each event individually [3]. This results in a PV position measurement with uncertainties of 7 μm transverse to the beam axis and 35 μm (52 μm for $b\overline{b}$ events) along the axis. The measured track impact parameter resolution is $\sigma_{r\phi}[\mu\text{m}] = 11 \oplus 70/p \sin^{3/2}\theta$, $\sigma_{rz}[\mu\text{m}] = 37 \oplus 70/p \sin^{3/2}\theta$, where $\oplus$ stands for the quadratic sum of the two terms and p is the track momentum expressed in GeV/c.

The hadronic event selection is based on charged track multiplicity and track visible energy requirements as described in Ref. [3]. The event selection is studied with Monte Carlo (MC) events generated using a JETSET 7.4 event generator [4], where the B hadron decays are simulated using a model tuned to current B and D decay data [5]. A plane transverse to the thrust axis is used to divide the event into two hemispheres. In order to ensure that the events are well contained within the acceptance of the VXD, the polar angle of the thrust is required to be within $|\cos\theta_{\text{thrust}}| < 0.71$. In addition, to ensure that the event hemisphere division is sensible and to reduce the contribution from events containing $g \to b\overline{b}$, we require that the event contain no more than three jets (defined using charged tracks and the JADE algorithm [6] with $y_{\text{cut}} = 0.02$). A total of 72 074 events were selected.

In each event, well-measured tracks [3] are used to search for a secondary vertex (SV). The SV are found by searching for areas of high track overlap density from the individual track resolution functions, in 3D coordinate space [7]. The SV are required to be separated from the PV by at least 1 mm and to contain at least two tracks each with a 3D impact parameter with respect to the IP $\geq$130 μm, ensuring that they originate from the decay of a particle with a relatively long lifetime. Simulation

studies show that secondary vertices are found in 50% of all b hemispheres, in 15% of the charm, and $<1\%$ of the light quark hemispheres [7]. The SV consists, on average, of 3.8 tracks.

Because of the cascade structure of the B decay, not all of the tracks in the decay chain will come from a common decay point, thus the SV is incomplete. We improve our estimate of the B decay vertex mass by attaching additional tracks to the SV which are consistent with the hypothesis of originating from the same SV. We illustrate this in Fig. 1(a). We define the vertex axis to be the straight line between the PV and SV centroids. For each track not in the SV, the 3D distance of closest approach T and the distance from the PV along the vertex axis to this point L are calculated. Tracks with $T < 1$ mm and $L/D > 0.25$, where D is the distance from the PV to the SV, are attached to the SV to form a B decay candidate. On average, 0.7 tracks are attached to the SV with the above algorithm; 82% of which come from the secondary and tertiary vertices, 6% come from the PV, and the remaining come from strange and long lived particles. The fraction of true prompt B decay tracks in the combined SV and attached B candidate tracks is 93%, while PV track fraction is 3%. The invariant mass $M_{\rm ch}$ of the B candidate is obtained by assuming each track has the mass of a charged π; the distribution of $M_{\rm ch}$ is shown in Fig. 2(a). If we require $M_{\rm ch}$ to be well above the charm mass, $M_{\rm ch} > 2\ \mathrm{GeV}/c^2$, it results in a b hemisphere tagging efficiency of 28% with a purity of 98%.

We improve the b tagging efficiency by applying a kinematic correction to the calculated $M_{\rm ch}$. Because of the neglect of information about the neutral particles in the decay, the SV flight path and the SV momentum vector are typically acollinear. In order to compensate for the acollinearity we correct $M_{\rm ch}$ using the minimum missing momentum (P_t) transverse to the SV flight path. To reject non-$b\bar{b}$ events with an artificially large P_t due to detector resolution effects, we define P_t with respect to a vector tangent to the error boundaries of both the PV and the SV, such that P_t is minimized [see Fig. 1(b)]. The ability to make this minimal correction is most effective at SLD due to the small and stable beam spot of the SLC and the high resolution vertexing. We then define the P_t-corrected mass, $\mathcal{M} = \sqrt{M_{\rm ch}^2 + P_t^2} + |P_t|$, and require $\mathcal{M} \leq 2 \times M_{\rm ch}$ to reduce the contamination from fake vertices in light quark events. The distribution of $\mathcal{M}$ is shown in Fig. 2(b). By requiring $\mathcal{M} > 2\ \mathrm{GeV}/c^2$ we significantly raise our b-tag efficiency, yielding $\epsilon_b = 35.3\%$ for the same purity.

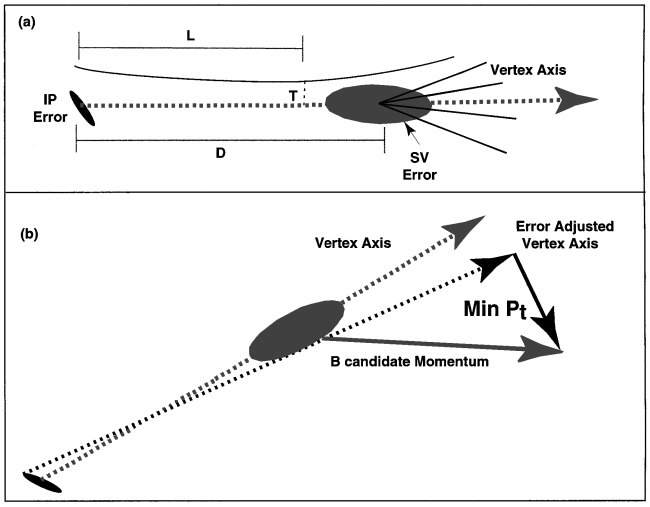

FIG. 1. (a) An illustration of the SV track attachment criteria. (b) Illustration of the P_t derivation.

We measure R_b and ϵ_b by counting the fraction of the event sample containing one tagged hemisphere, F_s, and the fraction containing both hemispheres tagged, F_d:

$$R_b = \frac{[F_s - R_c(\epsilon_c - \epsilon_{uds}) - \epsilon_{uds}]^2}{F_d - R_c(\epsilon_c - \epsilon_{uds})^2 + \epsilon_{uds}^2 - 2F_s\epsilon_{uds} - \lambda_b R_b(\epsilon_b - \epsilon_b^2)},$$

$$\epsilon_b = \frac{F_d - R_c\epsilon_c(\epsilon_c - \epsilon_{uds}) - F_s\epsilon_{uds} - \lambda_b R_b(\epsilon_b - \epsilon_b^2)}{F_s - R_c(\epsilon_c - \epsilon_{uds}) - \epsilon_{uds}}$$

The only term dependent upon B production and decay modeling is the b hemisphere tagging correlation, $\lambda_b = \frac{\epsilon_b^{\rm double} - \epsilon_b^2}{\epsilon_b - \epsilon_b^2} = 0.59\%$, where we have used the simulation to estimate λ_b. Estimates of the hemisphere tagging rates of light quarks, $\epsilon_{uds} = 0.06\%$, and charm quarks, $\epsilon_c = 0.69\%$, are also derived from the simulation, and we assume $R_c = \frac{\Gamma_{Z^0\to c\bar{c}}}{\Gamma_{Z^0\to q\bar{q}}} = 0.171$. We measure $R_b = 0.2142 \pm 0.0034_{\rm stat}$ which includes a correction of $+0.0003$ for the $e^+e^- \to \gamma \to b\bar{b}$ contribution as calculated by ZFITTER [8]. The measured value of $\epsilon_b = 35.3\% \pm 0.6\%$ is in good agreement with the MC estimate of 35.5%.

The systematic uncertainty on R_b, given in detail in Table I, results from a combination of detector related effects and physics uncertainties in the simulation which affect our estimates of ϵ_c, ϵ_{uds}, λ_b, and event selection bias. The physics systematic errors are assigned by comparing the nominal simulation distributions with an alternative set of distributions which reflect the uncertainties in the world average measurements of the MC physics parameters [9]. The two significant sources of systematic errors from light quark events come from the uncertainties in long lived strange particle production and gluon splitting into heavy quark pairs. The effects of strange particle production are studied by varying the $s\bar{s}$ production probability in jet fragmentation. The $g \to b\bar{b}$ and $g \to c\bar{c}$ production rates are varied based upon the OPAL $g \to c\bar{c}$

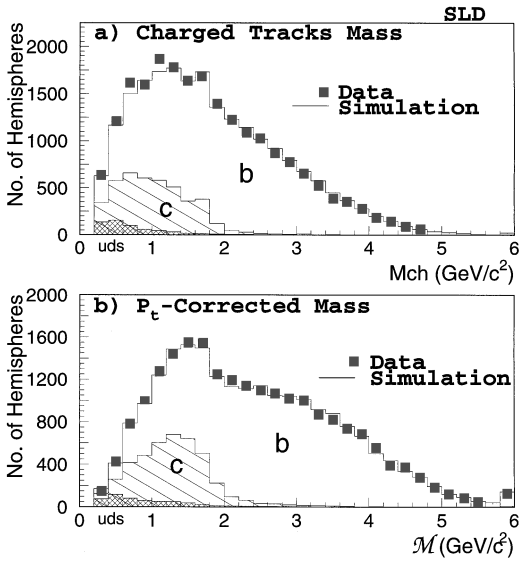

FIG. 2. Distribution of (a) $M_{\rm ch}$ and (b) P_t corrected mass $\mathcal{M}$ for data (points) and MC which includes a breakdown of the b, c, and uds contributions (open, hatched, and crosshatched histograms, respectively).

measurement [10] and the theoretical prediction for the ratio $g \to b\overline{b}/g \to c\overline{c}$ [9].

The various charmed hadron production rates and fragmentation parameters in Z^0 decays are varied within the present CERN Large Electron-Positron Collider (LEP) measurement errors. Charmed hadron fragmentation is studied by varying the average scaled energy $\langle x_E \rangle$ in the Peterson fragmentation function [11], as well as by studying the difference between the Peterson and Bowler models [12] for the same values of $\langle x_E \rangle$. Charmed hadron decay lifetimes are varied according to the world average measurement errors [13]. The charmed hadron decay charged multiplicity and K^0 production rate systematic uncertainties are based on measurements by Mark-III [14]. Charmed hadron decays with fewer neutral particles have higher charged mass and are therefore more likely to be tagged. Thus, an additional systematic uncertainty is estimated by varying the rates of charmed hadron decays with no $\pi^0 s$ by $\pm 10\%$.

The B production and decay modeling uncertainty enters via the λ_b estimation. It is studied by varying the B lifetime, B baryon production rate, B fragmentation function, and the B decay charged multiplicity in a manner similar to that for the charm systematic studies. Simulation uncertainties which affect the tagging efficiency are studied by comparing the angular distribution of the b-tagging rate between data and simulation, and a systematic error is assigned to the difference. Hard gluon radiation effects are estimated from a $\pm 30\%$ variation of the fraction of simulation events, where both B hadrons are contained within the same hemisphere and a hard gluon is in the other. Another systematic error is assigned to the effects of B hadron momentum correlation between the two hemispheres, due mainly to soft gluon radiation and fragmentation effects, which in turn translate to a b-tagging efficiency correlation. This is estimated by comparing the B momentum correlation in the HERWIG [15] and JETSET [4] event generators.

As a cross check, we decomposed the efficiency correlation into an independent set of components which represent all sources of correlation between the two b hemispheres. The components we have studied and their

TABLE I. Summary of systematic uncertainties for the $\mathcal{M} > 2.0\ \mathrm{GeV}/c^2$ cut.

Light Quark Systematic (ϵ_{uds})	δR_b
$g \to b\overline{b}$ 0.31 ± 0.11%	−0.00033
$g \to c\overline{c}$ 2.38 ± 0.48%	−0.00004
K^0 production ±10%	−0.00003
Λ production ±10%	−0.00002
Total uds physics systematic	**0.00034**
Charm Systematic (ϵ_c)	δR_b
D^+ production 0.259 ± 0.028	−0.00011
D_s production 0.115 ± 0.037	−0.00005
c-baryon production 0.074 ± 0.029	0.00011
c-frag. $\langle x_E \rangle_D = 0.482 \pm 0.008$	−0.00006
c-frag. function shape	−0.00001
D^0 lifetime 0.415 ± 0.004 ps	−0.00003
D^+ lifetime 1.057 ± 0.015 ps	−0.00001
D_s lifetime 0.467 ± 0.017 ps	−0.00002
Λ_c lifetime 0.200 ± 0.011 ps	−0.00001
D^0 decay $\langle N_{\rm ch} \rangle = 2.54 \pm 0.05$	−0.00006
D^+ decay $\langle N_{\rm ch} \rangle = 2.50 \pm 0.06$	−0.00006
D_s decay $\langle N_{\rm ch} \rangle = 2.65 \pm 0.33$	−0.00009
$D^0 \to K^0$ production 0.401 ± 0.059	+0.00015
$D^+ \to K^0$ production 0.646 ± 0.078	+0.00020
$D_s \to K^0$ production 0.380 ± 0.06	+0.00002
D^0 decay no-π^0 frac. 0.370 ± 0.037	+0.00005
D^+ decay no-π^0 frac. 0.499 ± 0.050	−0.00008
D_s decay no-π^0 frac. 0.352 ± 0.035	<0.00001
Total Charm Physics systematic	**0.00033**
B decay modeling (λ_b)	δR_b
B lifetime ±0.05 ps	0.00004
B decay $\langle N_{\rm ch} \rangle = 5.73 \pm 0.35$	0.00003
b fragmentation	0.00019
Λ_b production fraction 0.074 ± 0.03	0.00008
Hard gluon radiation	0.00008
B momentum correlation	0.00029
b-tag $\cos\theta$ dependency	0.00001
Total $b\overline{b}$ Physics systematic	**0.00038**
Detector Systematic	δR_b
Tracking resolution	0.00096
Tracking efficiency	0.00040
$\langle \mathrm{IP} \rangle_{xy}$ tail	0.00010
MC statistics	0.00053
Event selection bias	0.00071
Total detector and MC	**0.00137**
$R_c = 0.171 \pm 0.006$	**0.00021**
Total (excl. R_c)	**0.00150**

contributions are the PV measurement (-0.02%), the track resolution effect on the IP determination ($+0.04\%$), the detector nonuniformity via the tagging angular distribution dependence ($+0.49\%$), the momentum distribution of the B hadron in each hemisphere ($+0.08\%$), and the effect of hard gluon emission forcing the two B hadrons into one hemisphere ($+0.07\%$). The estimated λ_b $(0.59 \pm 0.11)\%$ and that from the sum of the components (0.67%) are in good agreement. The largest correlation component of detector nonuniformity is due mainly to the tagging efficiency dependence on $|\cos\theta|$, combined with the back-to-back nature of events. The source of this dependence is the variation of the effective thickness of detector material affecting track multiple scattering, which is well simulated by the MC and verified by comparing data and simulation for the hemisphere tag rate dependence on $\cos\theta$.

A major source of detector systematic uncertainty is due to the discrepancy in modeling the track impact parameter resolution, mainly along the beam axis. In the simulation track z impact parameters are smeared using a random Gaussian distribution of width $20\ \mu\text{m}/\sin\theta$, as well as being adjusted for z impact parameter mean position shifts to match the data. The full difference in R_b between the nominal and resolution-corrected samples is conservatively assigned to be the resolution systematic error. The difference between the measured and simulation charged track multiplicity as a function of $\cos\theta$ and momentum is attributed to an unsimulated tracking inefficiency correction. Both the tracking resolution and efficiency corrections require the use of a random number generator. After application of these corrections, the results vary slightly with different random sequences. These fluctuations are included as an additional MC statistical uncertainty. The uncertainty on the primary vertex x-y location simulation is estimated from the effect of adding a Gaussian tail to the IP distribution of 100 μm width for 0.5% of the simulated events.

The JETSET simulation [4] shows that the ≤ 3 jets requirement in the event selection favors $b\bar{b}$ over other $q\bar{q}$ events, which biases our measurement by $+0.55\%$. We verified this bias in the data, by measuring R_b with and without applying the ≤ 3 jet criterion, and found that our measured R_b value changed by only 0.0001, which is consistent with a statistical fluctuation. We have also examined the effect of the running mass of the b quark, m_b, on the above ≤ 3 jet cut. A systematic error is conservatively assigned to the effect of the full difference in calculated ≥ 4 jet b event rates compared between using the pole mass and using the running mass at M_Z for m_b [16]. Including the fragmentation and reconstruction effects, the resulting uncertainty on R_b due to bias introduced by the ≤ 3 jet requirement on event selection is 0.31%. Another bias of $+0.26 \pm 0.12\%$ is introduced by the other event selection criteria, thus the combined bias is $0.82 \pm 0.33\%$ and was corrected.

Finally, the $\mathcal{M}$ cut value of 2 GeV/c^2 was chosen to minimize the total statistics plus systematic uncertainties. Where the statistical error increases as the mass cut is increased, the charmed hadron systematic contribution, which dominates the R_b uncertainty at low values of $\mathcal{M}$ cut, drops rapidly as the mass cut is raised beyond the charmed hadron mass. As a cross check, we repeated the analysis using different $\mathcal{M}$ cuts, resulting in consistent R_b values for values of $\mathcal{M}$ between 0–3 GeV/c^2.

In summary, we have measured

$$R_b = 0.2142 \pm 0.0034(\text{stat}) \pm 0.0015(\text{syst}) \pm 0.0002(R_c)$$

which includes a correction of $+0.0003$ for the $e^+e^- \to \gamma \to b\bar{b}$ contribution. This value supersedes our previous R_b measurements [3] and is in good agreement with the SM prediction of 0.2158. A new high precision measurement has recently been reported by ALEPH [17], which also incorporates mass information to improve a lifetime-based probability tag. With the new SLD and LEP measurements, the gap between the SM prediction of R_b and the world average has narrowed.

We thank the personnel of the SLAC Accelerator Department and the technical staffs of our collaborating institutions for their outstanding efforts on our behalf. This work was supported by the U.S. Department of Energy and National Science Foundation, the UK Particle Physics and Astronomy Research Council, the Istituto Nazionale di Fisica Nucleare of Italy, the Japan-US Cooperative Research Project on High Energy Physics, and the Korea Science and Engineering Foundation.

*Deceased.
†Also at the Università di Genova, I-16146 Genova, Italy.
‡Also at the Università di Perugia, I-06100 Perugia, Italy.

[1] M. Hildreth, in *Electroweak Interactions and Unified Theories*, edited by J. Tran Than Van, Proceedings of XXXI Rencontres de Moriond (Editions Frontieres, Gif-sur-Yvette, France, 1996), p. 147.
[2] ALEPH Collaboration, D. Buskulic *et al.*, Phys. Lett. B **313**, 535 (1993); OPAL Collaboration, P. D. Acton *et al.*, Z. Phys. C **60**, 579 (1993); D. Akers *et al.*, Z. Phys. C **65**, 17 (1994); K. Ackerstaff *et al.*, Z. Phys. C **74**, 1 (1997); DELPHI Collaboration, P. Abreu *et al.*, Z. Phys. C **66**, 323 (1995); Z. Phys. C **70**, 531 (1996).
[3] SLD Collaboration, K. Abe *et al.*, Phys. Rev. D **53**, 1023 (1996).
[4] T. Sjostrand, Comput. Phys. Commun. **82**, 74 (1994).
[5] QQ MC code provided by P. Kim and the CLEO Collaboration. Tuning of the B decay modeling is described in SLD Collaboration, K. Abe *et al.*, Phys. Rev. Lett. **79**, 590 (1997).
[6] JADE Collaboration, S. Bethke *et al.*, Phys. Lett. B **213**, 235 (1988).
[7] D. Jackson, Nucl. Instrum. Methods Phys. Res., Sect. A **388**, 247 (1997).
[8] D. Bardin *et al.*, Report No. CERN-TH 6443/92, 1992.
[9] The LEP Electroweak Working Group, "Presentation of the LEP Electroweak Heavy Flavour Results for Summer

1996 Conferences," Report No. LEPHF/96-01, July 1996; http://www.cern.ch/LEPEWWG/heavy/lephf9601.ps.gz.
[10] OPAL Collaboration, R. Akers *et al.,* Phys. Lett. B **353**, 595 (1995).
[11] C. Peterson *et al.,* Phys. Rev. D **27**, 105 (1983).
[12] M. G. Bowler, Z. Phys. C **11**, 169 (1981).
[13] Particle Data Group, L. Montanet *et al.,* Phys. Rev. D **50**, 1173 (1994).
[14] Mark-III Collaboration, D. Coffman *et al.,* Phys. Lett. B **263**, 135 (1991).
[15] G. Marchesini *et al.,* Comput. Phys. Commun. **67**, 465 (1992).
[16] A. Santamaria and A. Brandenburg (private communication); G. Rodrigo, A. Santamaria, and M. Bilenky, Phys. Rev. Lett. **79**, 193 (1997); W. Bernreuther, A. Brandenburg, and P. Uwer, Phys. Rev. Lett. **79**, 189 (1997).
[17] ALEPH Collaboration, R. Barate *et al.,* Phys. Lett. B **401**, 150 (1997); **401**, 163 (1997).